(2) Coronary artery segments with substantial calcification may not be evaluable with respect to the presence of a hemodynamically relevant stenosis. (3) The coronary lumen is generally not well observed in the region of a coronary stent. In addition to these, the adverse effect of iodinated contrast media and risk for radiation exposure are common problems related to contrast-enhanced CT. The latter is highlighted in low-pitch helical mode cardiac CTA. Prospective ECG-triggered CTA, with low radiation exposure, is promising and any efforts to further optimize or reduce the dose should be made.

Conclusion

Prospective ECG-triggered CTA can markedly reduce the radiation dose, while maintaining diagnostic performance, in patients with low and stable heart rate. The suitable indication is exclusion of obstructive coronary disease and is most beneficial for young patients, who are at low risk of significant coronary artery disease.

Abbreviations

ECG: electrocardiograph
CT: computed tomography
CTA: computed tomography angiography
bpm: beats per minute
BMI: body mass index

References and Recommended Reading

Papers of particular interest, published recently, have been highlighted as:

* Of importance

** Of major importance

1. Abdulla J, Abildstrom SZ, Gotzsche O, et al. **64-multislice detector computed tomography coronary angiography as potential alternative to conventional coronary angiography: a systematic review and meta-analysis.** European Heart Journal 2007;**28**:3042-3050.

2. Budoff MJ, Dowe D, Jollis JG, et al. **Diagnostic performance of 64-multidetector row coronary computed tomographic angiography for evaluation of coronary artery stenosis in individuals without known coronary artery disease.** JACC 2008;**52**:1724-1732.

3. Meijboom WB, Meijs MF, Schuijf JD, et al. **Diagnostic accuracy of 64-slice computed tomography coronary angiography. a prospective, multicenter, multivendor study.** J Am Coll Cardiol 2008;**52**:2135-2144.

4. Einstein AJ, Moser KW, Thompson RC, et al. **Radiation dose to patients from cardiac diagnostic imaging.** Circulation 2007;**116**:1290-1305.

5. Ritchie CJ, Godwin JD, Crawford CR, et al. **Minimum scan speeds for suppression of motion artifacts in CT.** Radiology 1992;**185**:37-42.

6. Lu B, Mao SS, Zhuang N, et al. **Coronary artery motion during the cardiac cycle and optimal EKG triggering for coronary artery imaging.** Invest Radiol 2001;**36**:250-256.

7. Hoffmann MHK, Lessick J, Manzke R et al. **Automatic determination of minimal cardiac motion phases for computed tomography imaging: initial experience.** Eur Radiol 2006;**16**:365-373.

8. Cademartiri F, Mollet NR, Runza G, et al. **Improving diagnostic accuracy of MDCT coronary angiography in patients with mild heart rhythm irregularities using ECG editing.** AJR 2006;**186**:634-638.

9. Jakobs TF, Becker CR, Ohnesorge B, et al. **Multislice helical CT of the heart with retrospective ECG gating: reduction of radiation exposure by ECG-controlled tube current modulation.** Eur Radiol 2002;**12**:1081-1086.

10. Hausleiter J, Meyer T, Hadamitzky M, et al. **Radiation dose estimates from cardiac multislice computed tomography in daily practice: impact of different scanning protocols on effective dose estimates.** Circulation 2006;**113**:1305-1310.

11. Husmann L, Valenta I, Gaemperli O, et al. **Feasibility of low-dose coronary CT**

angiography: first experience with prospective ECG-gating. European Heart Journal 2008;**29**;191-197.
12. Petersilka M, Bruder H, Krauss B, Stierstorfer K, Flohr TG. **Technical principles of dual source CT.** European Journal of Radiology 2008;**68**:362-368.
13. Kimura F, Umezawa T, Shen Y, et al. **Coronary CT angiography using prospectively gated axial scans: evaluation of banding artifacts and padding time.** Presented at Radiological Society of North America 2008.
14. 1990 recommendations of the International Commission on Radiological Protection. ICRP Publication 60. Ann ICRP 1990;21
15. US Food and Drug Administration Center for Devices and Radiological Health. Whole body scanning using computed tomography (CT): what are the radiation risks from CT? Available at: www.fda.gov/cdrh/ct/risks.html. Accessed January 2009.
16. Committee to assess health risks from exposure to low levels of ionizing radiation, National Research Council. Nuclear and Radiation Studies Board. Health risks from exposure to low levels of ionizing radiation.2005. 2006. Washington, DC, The National Academies Press. Ref Type: Report.
17. Morin RL, Gerber TC, McCollough CH. **Radiation dose in computed tomography of the heart.** Circulation 2003;**107**:917-922.
18. Einstein AJ, Moser KW, Thompson RC, et al. **Radiation dose to patients from cardiac diagnostic imaging.** Circulation 2007;**116**:1290-1305.
19. Hunold P, Vogt FM, Schmermund A, et al. **Radiation exposure during cardiac CT: effective doses at multi-detector row CT and electron-beam CT.** Radiology 2003;**226**:145-152.
20. Achenbach S, Giesler T, Ropers D, et al. **Detection of coronary artery stenoses by contrastenhanced, retrospectively electrocardiographically-gated, multislice spiral computed tomography.** Circulation 2001;**103**:2535-2538.
21. Mollet NR, Cademartiri F, van Mieghem CA, et al. **High-resolution spiral computed tomography coronary angiography in patients referred for diagnostic conventional coronary angiography.** Circulation **2005**;112:2318–23.
22. Oncel D, Oncel G, Tastan A. **Effectiveness of dual-source CT coronary angiography for the evaluation of coronary artery disease in patients with atrial fibrillation: initial experience.** Radiology 2007;**249**:703-711.
23. Stolzmann P, Scheffel H, Schertler T, et al. **Radiation dose estimates in dual-source computed tomography coronary angiography.** Eur Radiol 2008;**18**:592-599.
24. * Hirai N, Horiguchi J, Fujioka C, et al. **Prospective**

electrocardiography-triggered versus retrospective electrocardiography-gated 64-slice coronary CT angiography: image quality, stenoses assessment and radiation dose. Radiology 2008;**248**:424-430.
This study shows the comparability of prospective ECG-triggered to ECG-modulated retrospective ECG-gated 64-slice CTA as regards image quality and stenoses assessment in the same patients (n=60), while dose reduction by 79%.
25. Shuman WP, Branch KR, May JM, et al. **Prospective versus retrospective ECG gating for 64-detector CT of the coronary arteries: comparison of image quality and patient radiation dose.** Radiology 2008;**248**:431-437.
26. ** Maruyama T,Masanori Takada M, et al. **Radiation dose reduction and coronary assessability of prospective electrocardiogram-gated computed tomography coronary angiography.** J Am Coll Cardiol 2008;**52**:1450-1455.
An important study shows that prospective ECG-triggered 64-slice CTA (n=76) has equivalent coronary assessability and diagnostic accuracy in comparison with ECG-modulated retrospective ECG-gated CTA (n=97) with decreased radiation dose by 79% reduction.
27. Earls JP, Berman EL, Urban BA, et al. **Prospectively gated transverse coronary CT angiography versus retrospectively gated helical technique: improved image qualityand reduced radiation dose.** Radiology 2008; **246**:742-753.
28. Herzog BA, Husmann L, Burkhard N, et al. **Accuracy of low-dose computed tomography coronary angiography using prospective electrocardiogram-triggering: first clinical experience.** European Heart Journal 2008;**29**:3037-3042.
29. * Scheffel H, Alkadhi H, Leschka S, et al. **Low-dose CT coronary angiography in the step-and-shoot mode: diagnostic performance.** Heart 2008;**94**:1132-1137.
This article investigates the diagnosis of significant coronary artery disease on prospective ECG-triggered dual-source CTA in 120 patients, compared to invasive angiography.
30. Stolzmann P, Leschka S, Scheffel H, et al. **Dual-source CT in step-and-shoot mode: noninvasive coronary angiography with low radiation dose.** Radiology 2008; **249**: 71-80.
31. Alkadhi H, Stolzmann P, Scheffel H, et al. **Radiation dose of cardiac dual-source CT: the effect of tailoring the protocol to patient-specific parameters.** European Journal of Radiology 2008;**68**:385-391.
32. Rybicki FJ, Otero HJ, Steigner ML, et al. **Initial evaluation of coronary images from 320-detector row computed tomography.** Int J Cardiovasc Imaging

2008;**24**:535-546.
33. Ertl-Wagner BB, Hoffmann RT, Bruning R, et al. **Multi-detector row CT angiography of the brain at various kilovoltage settings.** Radiology 2004;**231**:528-535.
34. Abada HT, Larchez C, Daoud B, et al. **MDCT of the coronary arteries: feasibility of low-dose CT with ECG-pulsed tube current modulation to reduce radiation dose.** AJR 2006;**186**:S387-390.
35. Deetjen A, Mo¨llmann S, Conradi G, et al. **Use of automatic exposure control in multislice computed tomography of the coronaries: comparison of 16-slice and 64-slice scanner data with conventional coronary angiography.** Heart 2007;**93**:1040-1043.
36. Bluemke DA, Achenbach S, Budoff M, et al. **Noninvasive coronary artery imaging: magnetic resonance angiography and multidetector computed tomography angiography: a scientific statement from the American Heart Association Committee on Cardiovascular Imaging and Intervention of the Council on Cardiovascular Radiology and Intervention, and the Councils on Clinical Cardiology and Cardiovascular Disease in the Young.** Circulation 2008;**118**:586-606.
37. Horiguchi J, Kiguchi M, Fujioka C, et al. **Radiation dose, image quality, stenosis measurement, and CT densitometry using ECG-triggered coronary 64-MDCT angiography: a phantom study.** AJR 2008;**190**:315-320.
38. Gutstein A, Wolak A, Lee C, et al. **Predicting success of prospective and retrospective gating with dual-source coronary computed tomography angiography: development of selection criteria and initial experience.** J Cardiovasc CT 2008;**2**:81-90.

Figure 1

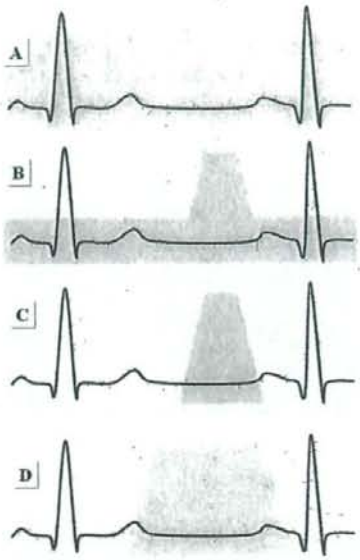

Figure 2

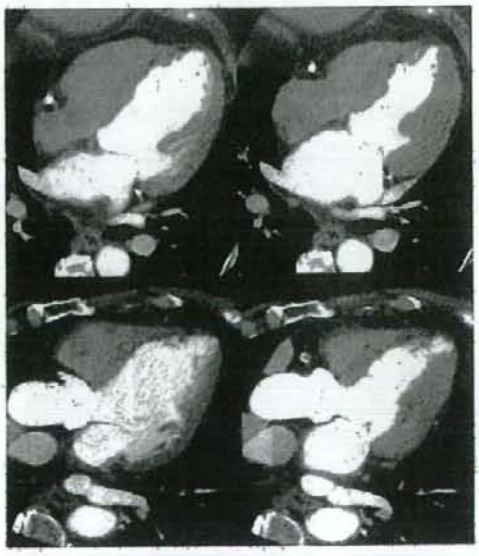

Figure 3

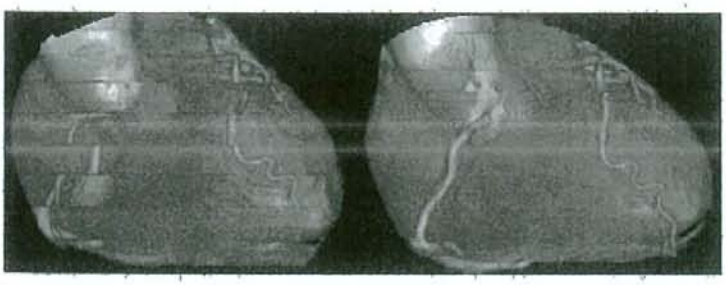

Figure 4A

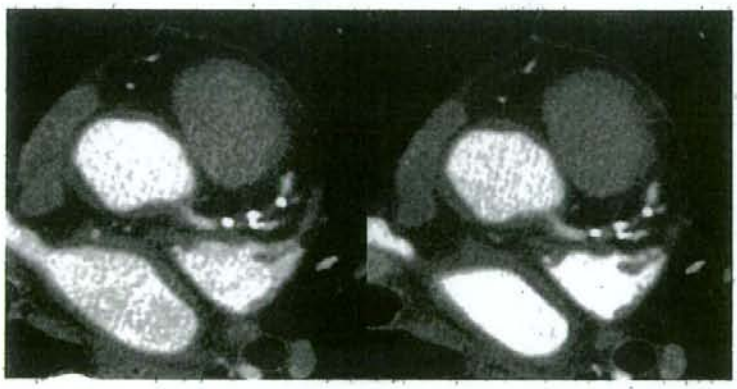

Figure 4B

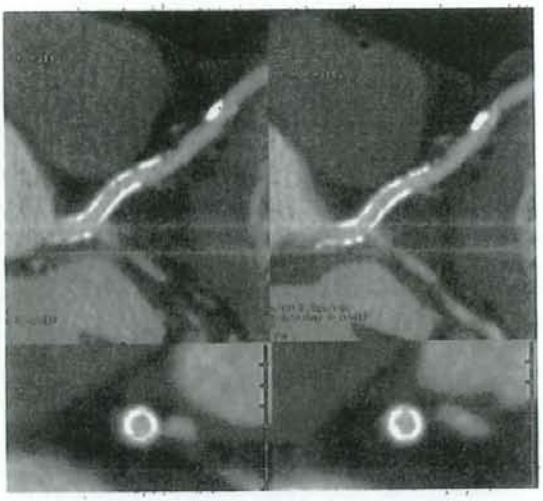

Figure 5

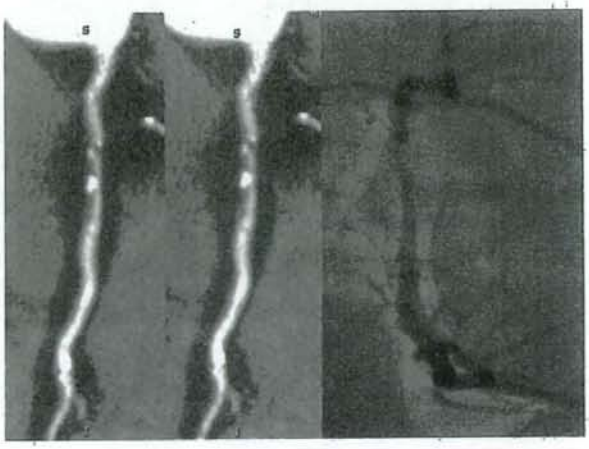

Table

Effective Dose of Cardiac Examination

Diagnostic modality	Effective dose (mSv)	Reference No.
Radioisotope		
Diagnostic coronary angiogram	3–10*	17
99mTc sestamibi rest-stress	11.3*	18
99mTc sestamibi stress only	7.9*	18
201Tl stress-redistribution	22*	18
201Tl stress-reinjection	31.4*	18
Dual isotope 201Tl-99mTc sestamibi	29.2	
Calcium Scoring with Electron-Beam CT	1-1.3	19
Retrospective ECG-gated CTA		
4-slice CTA	3.9-5.8	20
64-slice CTA	15.2–21.4	21
Dual-source CT	13.8	22
ECG-modulated 64-slice CTA	9	10
ECG-modulated dual-source CT	7-9	23
Prospective ECG-triggered CTA		
Electron beam CTA	1.5-2	19
64-slice CTA	4.1-4.3	24-26
64-slice CTA (100 kV and 120 kV)	2.1-2.8	11, 27-29
Dual-source CTA	2.6-2.9	30,31
Dual-source CTA, 100 kV	1.2-1.3	30,31
320-slice CTA	6.8**	32

* The effective dose estimated from tissue dose coefficients, using ICRP Publication 60 tissue weighting factors.

** The phase window was set to 60–100% of RR interval.

Figure legends

Figure 1 Prospective ECG-triggered versus Retrospective ECG-gated Techniques

A: Conventional retrospective ECG-gated scan is performed in the spiral mode using a fixed tube current throughout cardiac cycle.
B: ECG-modulated retrospective ECG-gated scan reduces the tube current during a particular part of the cardiac cycle (usually systole), allowing for a reduction of the radiation dose by 30% to 50%.
C: Prospective ECG-triggered scan applies radiation during short and predetermined acquisition window of the cardiac cycle, thereby reducing the radiation dose by around 80%, compared to the retrospective ECG-gated scan.
D: X-ray exposure in prospective ECG-triggered scan can be elongated to increase additional reconstruction availability. It enables the accommodation of some heart rate variation, however, at the expense of increased radiation exposure.

Figure 2 Wall Motion Evaluation on Retrospective ECG-gated Technique

59 yo female with previous history of myocardial infarction
Upper panels show two-chambers view and lower three-chambers view. Left panels indicate diastolic phase and right systolic. The apicoseptal wall shows thinning and endocardial fat deposition, associated with segmentally decreased wall motion. The wall of the proximal right coronary artery is calcified and the lumen is not enhanced.

Figure 3 ECG Editing Technique

The heart rate with a patient presenting arrhythmia ranged 34 to 145 bpm. The reconstruction at 75% of RR shows marked stair-step (i.e. banding) artifacts (left panel). The image misregistration is reduced after applying ECG-editing technique (right).

Figure 4 Comparison of Prospective ECG-triggered versus Retrospective ECG-gated Images

A: 78 yo male complaining of recent myocardial infarction (Agatston score: 350 units). Prospective ECG-triggered (left panel, 60 bpm) and retrospective ECG-gated (right, 61 bpm) images show comparable image quality.
B: 65 yo male, with 3.5mm DRIVER stent implanted in the left main coronary artery, complaining of indeterminate chest pain.
Similarly on both scans (prospective ECG-triggered; left panel, 57 bpm, retrospective ECG-gated; right, 58 bpm), the patency of the stent can be confirmed on curved multiplanar reconstruction views along long and short axes of the stent.

Figure 5 Comparison of Prospective ECG-triggered and Retrospective ECG-gated Images versus Invasive Angiography

62 yo male complaining of progressive effort angina
Curved multiplanar reformation images of prospective ECG-triggered (left panel) and retrospective ECG-gated (middle) images show severe stenosis caused by complex (calcified and non-calcified) plaque. Angiography shows 90% stenosis at the proximal right coronary artery.

Radiology, in submission

Title

Attenuation-Based Tube Current Control in Coronary Artery Calcium Scoring on Prospective ECG-triggered 64-Detector CT

Abstract

Purpose

To optimize image noise (standard deviation of CT value) and to assess variability in repeated coronary artery calcium (CAC) scoring on prospective electrocardiograph (ECG)-triggered 64-multidetctor CT (MDCT).

Materials and Methods

This prospective study was approved by our institutional review committee. Patients (n=428) suspected of coronary artery disease were scanned twice using each of three protocols; the tube current modified by Group A: body mass index (BMI), Group B: BMI and body height and Group C: attenuation at the maximal heart diameter. Image noise was plotted against BMI. Interscan variability of CAC scores was obtained. The effective dose was estimated by CT dose index.

Results

The mean effective dose and image noise were Group A: 0.9±0.2(range, 0.6-1.5) mSv and 19±4(10-32) HU, Groups B: 0.8±0.2(0.5-1.4) mSv and 18±4(10-31) HU and Group C: 0.8±0.4(0.3-2.2) mSv and 20±2(16-26) HU. Group C used a wide range of dose and controlled the noise in a small range. The positive slope of image noise/ BMI, 0.81 HU/(kg/m^2) in Group A and 0.62 HU/(kg/m^2) in Group B, suggested insufficient control of the tube current. In contrast, the nearly flat slope; 0.091 HU/(kg/m^2) in Group C, indicated optimal control. The interscan variability for Agatston, volume and mass in CAC positive patients (n=300) was 13%(median, 8%), 12%(7%) and 11%(6%), respectively.

Conclusion

Attenuation-based tube current control has the potential to optimize image noise. Low-dose and low interscan variability on CAC scoring are shown on prospective ECG-triggered 64-MDCT.

Introduction

The validity of serial coronary calcium measurements as a method to monitor progression of atherosclerosis requires: 1) that progression of CAC has biologic relevance to atherosclerosis activity; 2) that progression of CAC can be detected relative to inter-test variability; 3) that changes in CAC severity have prognostic relevance; and 4) that modification of cardiovascular risk factors modulates the progression of CAC [1]. Therefore, regarding as technical aspects of CAC scoring, low radiation exposure and low interscan variability are key requirements.

To reduce radiation exposure, a lower tube current time product of 40mAs [2] or 55 mAs [3] has been recommended for low-dose CAC scoring. However, scanning using a fixed tube current does not account for body habitus of patients. In a recent report of the International Consortium on Standardization in Cardiac CT, a SD level target of 20 HU for small and medium-size patients and a SD level target of 23 HU for large patients have been recommended [4]. To adjust tube current individually, body weight-adapted [5-7] or BMI-adapted [8,9] protocols have been introduced. However, even in these models, neither the size of heart nor the presence of pericardial effusion is considered [10]. Mühlenbruch et al. reported automated attenuation-based tube current adaptation where the tube current was chosen from a proprietary control curve calculated based on the attenuation values derived from the scanogram [10]. The effective reference mAs; i.e. 150 mAseff, 180 mAseff or 201 mAseff on spiral scan, was set constant for all z-axis positions. Their study showed automated attenuation-based tube current adaptation can better optimize tube current than a fixed 'standard' dose protocol, however, they admitted that the regression analysis revealed statistically significant influence of patient's BMI on image noise. We hypothesized that the tube current should be adjusted by attenuation at the level of maximal heart diameter on the scout, i.e. the z-axis level used for the calculation of cardiothoracic ratio. Moreover, step-and shoot scan should be used for the reduction of radiation dose. Thus, the main purpose of this prospective study was to optimize image noise and to assess variability in repeated CAC scoring on prospective ECG-triggered 64-MDCT using attenuation-based tube current adaptation at the maximal heart diameter. We also compared this protocol with two other protocols; tube current modified by body BMI [9] and tube current modified by BMI and body height.

Materials and methods:

Patients

The study was approved by our institutional review committee. Written informed consent was received from all patients involved after the nature of the procedure had been fully explained (including radiation dose information). For 24 months, 428 consecutive subjects (261 males and 167 females, 65±12 years old: ranged, 28-89 years) who underwent coronary CT for coronary risk factors or chest pain evaluation were enrolled in the study and were classified into three groups. Patients with a history of cardiac surgery, stents or a pacemaker were excluded. Study participants were collected until each group reached 100 patients with CAC.

Prospective ECG-Triggered Step and Shoot CT Protocol

Two-repeated prospective ECG-triggered step-and-shoot half-scans were performed using a 64-MDCT scanner (LightSpeed VCT; GE Healthcare, Waukesha, WI, USA) with simultaneous ECG digitizing and recording. Between the two scans, in order to simulate different body positions, the table was advanced by 1mm. Scans were performed 4 to 5 seconds after holding the breath on mild inspiration in order to minimize change of heart rate during the scan [11]. Using 2.5 mm collimation width x 16 detectors, images of 2.5 mm thickness were obtained. Scans were temporally triggered to be centered at 75% RR, as mid-diastole reconstruction has been recommended on 0.35 sec gantry-rotation-speed 64-MDCT scanner [12]. The gantry rotation speed was 0,35 sec/rotation and the tube voltage 120 kV. For image reconstruction parameters, a matrix size of 512 x 512 pixels, display field of view of 26cm and the kernel 'Standard' were used. The temporal resolution was 175 msec.

Group A: tube current modified by BMI

This group consisted of subjects in a formerly published paper [9] plus 20 subjects. As a significant association between noise and BMI was shown in an electron beam CT study [8], the tube current was modified according to the following equation:

Tube current = 250 x (body mass index / 25) mA

$= 10 \times \text{body weight (kg)} / [\text{body height (m)}]^2$ mA

This is based on the strategy that patients with a standard body mass index of 25 kg/mm^2 receive the tube current time product of 58 mAs, which is almost the same level as the recommendation in CAC scoring on low dose 4-slice CT [3].

The tube current time product in a typical patient with a BMI of 25 kg/m^2
= tube current (mA) x gantry rotation speed (sec) x exposure time per rotation time
=250 mA x 0.35 sec x 2/3 = 58 mAs

Group B: tube current modified by BMI and body height

In addition to BMI, the protocol considered the influence of body height. The tube current was modified according to the following equation:
Tube current = 250 x (body mass index / 25) mA x (body height / 1.7) mA
= 5.88 x body weight (kg) / [body height (m)] mA

Group C: attenuation-based tube current adaptation at the maximal heart diameter

As this protocol used attenuation-based tube current adaptation, we set the isocenter of X-ray beam to adjust the center of body in the ventral-dorsal direction at the left ventricular level. First, we took the lateral scout and, if necessary, reset the position of the table so that the isocenter of X-ray beam and the center of body correspond (Fig 1a). Next, we took the frontal scout. We determined the z-axis level of the maximal heart diameter on the frontal scout view (Fig 1b) and inputted a targeted noise level of 20 HU in software 'Smart mA', thereafter a value of tube current was recommended. As this value was offered on the simulation of a full scan and a gantry rotation speed of 0.4 sec, we determined the tube current on the CAC scanning according to the following equation:
Tube current = recommended tube current x 3/2 x (0.4/0.3) mA
= recommended tube current x 1.71 mA

Image Noise

Image noise expressed as standard deviation (SD) of CT values, in regions of interest set in the aorta at the level of the left coronary artery and in the right ventricle at the maximal heart diameter level determined on axial CT image, was measured by Observer1 (9 years' experience of CAC scoring) on Scan1 (Fig 2). The SD value in the right ventricle of each of the three groups was tested for being equal to 20HU. The value (mean + 2 x SD) of CT values, in the two regions of interest, which is preferably lower than the threshold of 130 HU [2], was calculated. To investigate the relationship between SD and BMI, the SD was plotted versus the BMI, as described by Mahnken et al [13].

Calcium Scoring

The Agatston [14], calcium volume and mass [15] were determined on a commercially available external workstation (Advantage Windows Version 4.2, GE Healthcare, Waukesha, WI) and CAC-scoring software (Smartscore Version 3.5).

All CT scans were independently scored by two radiologists with 9 and 3 years' experience of CAC scoring (Observer1 and Observer2, respectively). We defined 'CAC positive' as positive CAC scores for the three algorithms on both scans. For 'CAC positive' patients, the CAC scores in logarithmic scale, in order to reduce skewness, were compared between the three groups, as well as between two repeated scans and two observers. We performed monthly scanning of a calibration phantom (Anthropomorphic Cardio Phantom, Institute of Medical Physics, and QRM GmbH) to determine the calibration factor for mass score [16].

Interscan and Interobserver Variability

For 'CAC positive' patients, interscan and interobserver variability was calculated using the percentage difference in calcium scores:

Interscan variability = [absolute (Scan1 – Scan2) / (Scan1 + Scan2) x 0.5] x 100

Interobserver variability

= [absolute (Observer1 – Observer2) / (Observer1 + Observer2) x 0.5] x 100

where Observer1 is the CAC score measured by Observer1.

The interscan variability, in logarithmic scale, was compared between the three groups and CAC scoring algorithms.

Radiation dose

Dose-length product (DLP, in mGy x cm) displayed on Dose Report on the CT scanner was recorded. The effective dose was estimated by a method proposed by the European Working Group for Guidelines on Quality Criteria in CT [17]. In this method, the effective dose is derived from the dose-length product and a conversion coeffcient for the chest (k = 0.017 mSv/mGy per cm averaged between male and female models). The effective doses in the three groups were plotted versus the BMI.

Statistical Analyses

All statistical analyses were performed using a commercially available software

package (MedCalc 9.5.1 for Windows, Medcalc Software, Mariakerke, Belgium). Categorical variables were presented as frequency and percentage and continuous variables are as mean ± SD. The chi-square and ANOVA (multivariate calculations) tests were used to determine group differences. P-values < 0.05 were considered to identify significant differences.

Results

The patient numbers in Groups A, B and C were 145, 145 and 138, respectively. All patients (n=428) were able to hold their breath on the two scans. Baseline characteristics of patients are presented in Table 1. Neither heart rate (p=0.47) nor heart rate variation (p=0.44) was different between the three groups. Three hundred of the overall 428 patients were 'CAC positive'. One hundred and twenty patients showing negative scores on both scans, and 8 patients showing both positive and negative scores between scans or between algorithms, were excluded for the calculation of variability.

Image Noise

The SD and the values of (mean + 2 x SD) in regions of interest in the aorta and the right ventricle are presented in Table 2. The test for one mean revealed that the SD in the right ventricle was different from 20HU in Group A (p<0.01, 95% confidence interval [CI]: 18.3 to 19.7) and Group B (p<0.01, 95% CI: 17.3 to 18.7), whereas the SD was not different from 20HU in Group C (p=1.00, 95% CI: 19.7 to 20.3). In Group C, the mean SD was 20±2 HU, being controlled in a range from 16 HU to 26 HU. Images with the highest noise in the three groups are shown in Figure 3. In Group C, 6 of 138 patients (4%) showed CT value of >23HU in the right ventricle (at the maximal heart diameter level on axial CT image). In 5 patients of them, the image levels were below the dome of diaphragm, being different from the image used for the measurement of attenuation in the scout.

The values of (mean + 2 x SD) did not exceed 130 HU in Groups A and C, whereas the value, in the right ventricle, was 133 HU in one case in Group B.

The regression analysis revealed statistically significant influence of patient's BMI on the image noise in Groups A and B (Fig 4a-d). In Group C however, the nearly flat slopes of 0.04 HU/(kg/m^2) and 0.091 HU/(kg/m^2) were seen between the BMI on the SD, indicating optimal control of tube current (Fig 4e, f).

The CAC scores and the interscan and interobserver variability are summarized in Table 3. The CAC score levels were not different between the three groups. For a representative, one-factor ANOVA revealed that there was no significant difference of log transformed Agatston scores on Scan1 measured by Observer1 between the groups ($p=0.61$). CAC scores were not different between scans and observers; for an example, repeated measures ANOVA revealed that there was no statistical significance of log transformed Agatston scores in Group A between the scans ($p=0.31$) and observers ($p=0.91$).

For Observer 1, the mean interscan variability of 'CAC positive' patients in all groups ($n=300$) was Agatston: 13% (median; 8%), volume: 12% (7%) and mass: 11% (6%), respectively. Two-factor ANOVA revealed that the interscan variability in CAC scores, in logarithmic scale, was not different between the three groups ($p=0.17$) and algorithms ($p=0.07$).

The interobserver variability was small. For Scan1, the mean interobserver variability for Agatston, volume and mass in 'CAC positive' patients was 4% (1%), 2% (0%) and 3% (1%), respectively.

Radiation dose

The tube current, tube current time product, DLPs displayed on Dose Report on the CT scanner and the estimated effective doses, in the three groups, are shown in Table 4. One-factor ANOVA revealed that there was significant difference in all values between the three groups ($p<0.01$). Group C used the least dose, more importantly, a wide range of dose (effective dose: 0.3-2.2 mSv). The effective dose plots against the BMI are shown (Fig 5a-c). In Group C, the tube currents used and radiation doses were different between individuals, and widely distributed compared to Groups A and B.

Discussion

The major points of present study are (1) attenuation-based tube current control, at the level of maximal heart diameter on the scout view, has the potential to optimize image noise in CAC scoring. (2) Low-dose scan is possible in the combination of prospective ECG-triggered scan. (3) The protocol on 64-MDCT provides low interscan and interobserver variability.

Image Noise

In Group C, the mean noise was controlled to planned value of 20 HU. In addition,

the range was small compared to Groups A and B. These facts indicate that the scan in Group C keeps to 'as low as reasonably achievable (ALARA)' strategy. Of 138 patients in Group C, the maximal value of (mean + 2 x SD) was 107 HU in the right ventricle. As the CT value threshold of CAC detection was set to 130HU, this result indicates the noise is not likely to be falsely judged as CAC. This is also important as image noise is known to be one factor affecting interscan variability of CAC [18,19]. In Groups A and B, image noise was a function of BMI, suggesting insufficient control of the tube current to individual patient. In Group C however, image noise was in optimal control.

Interscan and Interobserver Variability in Coronary Artery Calcium Scoring

The interscan variability of Agatston score in 300 'CAC positive' patients (mean; 13% and median; 8% for Observer 1) was lower than the variability on electron beam CT (20% to 37%) [15,18,20,21] and was comparable to overlapping images from retrospective reconstruction on prior-generation (4- or 16-) MDCT [22,23]. The variability was also comparable to that on 64-MDCT [24]. However, the data on 64-MDCT are from a single institution. It is our hope that larger data from multi-institutions will be collected. Apart from overlapping images, the use of volume or mass algorithm can further reduce the variability. Although not significant ($p=0.07$), the trend was observed in the current study, in line with previous studies [23,24]. The interobserver variability in the study was small. Artificial lesions, known to affect interobserver variability, were reduced in the study with favorably controlled noise. We consider that the interscan and interobserver variability in the current study is encouraging. However, we might be prudent in real clinical practice, as patient is likely to have different heart rates when studies are performed a few years apart and body habitus and position may also change, thus possibly may increase variability.

Radiation dose

In Group C, the tube currents and the associated radiation doses distributed over a wide range and that the doses were different among patients even with the same BMI level. The attenuation-based tube current control is an appropriate method in patients who do not require much dose, e.g. a slender patient who does not receive more dose than necessary. For an example, the minimal dose was only 0.3 mSv for a small and slender patient (151cm, 42kg and BMI: 18 kg/m^2). We also found that the mean radiation dose in Group C was the same level as electron beam CT (0.7 mSv) [25]. We may therefore conclude that this level of radiation dose may be suited for repeated examination of monitoring progression of atherosclerosis. Another approach for the reduction of dose is lowering of the tube voltage [26,27]. It dose however, need calibration for the calculation of a scanner with a specifically adapted threshold for the

identification of calcium, and is available only for calcium mass scoring.

A technical issue should be addressed. As the current is determined at the maximal heart diameter on the scout, image noise below the dome of diaphragm tended to become higher. Indeed, 5 patients showed CT value of >23HU in the right ventricle below the dome of diaphragm. However, considering that the largest part of the coronary arteries was suggested to exist in the first 6 cm of the transverse scan [28], CAC below the diaphragmatic level is probably of less importance. Although we could have optimized the image noise adjusting at such a lower level, we did not choose to do so as it might excessively increase radiation dose.

As a limitation, the study was held at a single institution in Japan and the participants consisted of smaller patients than typical U.S. citizens, resulting in lower estimated dose than expected for U.S. citizens. Nevertheless, the method is applicable to any patients and seems promising for the optimization of the tube current in CAC scoring.

In conclusion, attenuation-based tube current control, at the level of maximal heart diameter on the scout view, has the potential to optimize image noise across patients. Low-dose and low interscan variability on CAC scoring are shown on prospective ECG-triggered 64-MDCT.

Acknowledgements

This study was financially supported by Tsuchiya Foundation (http://www.tsuchiya-foundation.or.jp), Hiroshima, Japan.

Abbreviations
CT: computed tomography
CAC: coronary artery calcium
MDCT: multidetector computed tomography
BMI: body mass index
SD: standard deviation
ECG: electrocardiograph
HU: Hounsfield unit
ANOVA: analysis of variance
DLP: dose-length product